Behavioral/Cognitive

The role of hippocampal-vmPFC neural dynamics in building mental representations

Anna M. Monk[1], Marshall A. Dalton[2], Gareth R. Barnes[1], Eleanor A. Maguire[1]

[1]Wellcome Centre for Human Neuroimaging, UCL Queen Square Institute of Neurology, University College London, 12 Queen Square, London WC1N 3AR, UK

[2]Sydney Imaging, Brain and Mind Centre, University of Sydney, Sydney, Australia

Abbreviated title: Building scene representations

Corresponding author: Eleanor Maguire; e.maguire@ucl.ac.uk

Number of pages: 32
Number of figures: 4
Number of tables: 1
Number of words in the Abstract: 245
Number of words in the Introduction: 649
Number of words in the Discussion: 1432

Acknowledgements: This work was supported by a Wellcome Principal Research Fellowship to E.A.M. (210567/Z/18/Z) and the Centre by a Centre Award from the Wellcome Trust (203147/Z/16/Z). We are grateful to the attendees of the MEG meetings at the Wellcome Centre for Human Neuroimaging at UCL for their advice. Thanks also to Daniel Bates, David Bradbury and Eric Featherstone for technical support.

The authors declare no competing financial interests and no conflicts of interest.

Abstract

The hippocampus and ventromedial prefrontal cortex (vmPFC) play key roles in numerous cognitive domains including mind-wandering, episodic memory and imagining the future. Perspectives differ on precisely how they support these diverse functions, but there is general agreement that it involves constructing representations comprised of numerous elements. Visual scenes have been deployed extensively in cognitive neuroscience because they are paradigmatic multi-element stimuli. However, it remains unclear whether scenes, rather than other types of multi-feature stimuli, preferentially engage hippocampus and vmPFC. Here we leveraged the high temporal resolution of magnetoencephalography to test human female and male participants as they gradually built scene imagery from three successive auditorily-presented object descriptions and an imagined 3D space. This was contrasted with constructing mental images of non-scene arrays that were composed of three objects and an imagined 2D space. The scene and array stimuli were, therefore, highly matched in terms of content and the associative and constructive processes they evoked. Across the three construction stages, we observed scene-related modulation of theta power in anterior hippocampus during the initial stage, and in vmPFC during the first two stages, relative to array construction. Moreover, the scene-specific anterior hippocampal activity during the first construction stage was driven by the vmPFC, with mutual entrainment between the two brain regions thereafter. These findings suggest that hippocampal and vmPFC neural activity seems to be especially tuned to scene representations, with implications for theories of how these brain areas operate and enable cognitive functions such as episodic memory.

Significance Statement

The hippocampus and ventromedial prefrontal cortex (vmPFC) play key roles in numerous cognitive domains. It has been suggested they might be especially tuned to building scene representations, which may be the smallest functional units of extended mental events like episodic memories. To test this, we used a mental imagery paradigm during magnetoencephalography whereby different tasks were closely matched for associative processing and mental construction, but either did or did not evoke scene representations. We observed preferential engagement of anterior hippocampus and vmPFC for building scenes, particularly at the beginning of construction, with the process being orchestrated by vmPFC. These findings may have implications for theories of how these brain areas operate and enable cognitive functions such as episodic memory.

Introduction

The hippocampus plays a key role in episodic memory (Scoville and Milner, 1957), spatial navigation (O'Keefe and Dostrovsky, 1971), and a range of other cognitive domains (reviewed in Clark and Maguire, 2016 and McCormick et al., 2018). Perspectives differ on precisely how the hippocampus supports these diverse cognitive functions. Nevertheless, there is general agreement that its contribution involves constructing representations comprised of numerous elements (Cohen and Eichenbaum, 1993; Lee et al., 2005; Hassabis and Maguire, 2007; Schacter and Addis, 2007; Yonelinas et al., 2019). Visual scenes have been deployed extensively to test hippocampal function because they are paradigmatic multi-element stimuli. A scene is defined as a naturalistic three-dimensional spatially-coherent representation of the world typically populated by objects and viewed from an egocentric perspective (Maguire and Mullally, 2013; Dalton et al., 2018).

Patients with hippocampal damage show scene-related perceptual, imagination and mnemonic impairments (Lee et al., 2005; Hassabis et al., 2007a; Mullally et al., 2012; Aly et al., 2013), and functional MRI (fMRI) studies have pinpointed the anterior hippocampus in particular as being engaged during scene perception and imagination (Hassabis et al., 2007b; Graham et al., 2010; Zeidman et al., 2015a, 2015b; Hodgetts et al., 2016; Zeidman and Maguire, 2016). Lesions to another brain region closely connected to the hippocampus (Catani et al., 2012, 2013), the ventromedial prefrontal cortex (vmPFC), also adversely affect scene imagination (Bertossi et al., 2016). Moreover, a recent magnetoencephalography (MEG) study showed that imagining scenes in response to single cue words (e.g. "jungle") was associated with theta power changes in anterior hippocampus and vmPFC, with the latter driving activity in the hippocampus (Barry et al., 2019).

Nevertheless, it remains unclear whether scenes, rather than other types of multi-feature stimuli, preferentially engage hippocampus and vmPFC. This is important to know because it directly informs theories of how the hippocampus and vmPFC operate and, as a consequence, how they enable cognitive functions such as episodic memory. One account posits that scenes are preferentially processed by the hippocampus and vmPFC, with vmPFC driving hippocampal activity (McCormick et

al., 2018; Ciaramelli et al., 2019; Barry and Maguire, 2019a, 2019b) whereas other views argue that it is the associating of multiple elements that requires hippocampal input, irrespective of whether scenes are the outcome of such processing (Cohen and Eichenbaum, 1993; Yonelinas et al., 2019).

To help adjudicate between these perspectives, here we adapted an fMRI paradigm which involved building scene imagery from three successive auditorily-presented object descriptions and imagining them in a 3D space (Dalton et al., 2018). This was contrasted with constructing images of non-scene arrays that were composed of three objects and a 2D space. The scene and array stimuli were, therefore, highly matched in terms of content and the associative and mental constructive processes they evoke. Focussing on the medial temporal lobe and averaging across the full imagery construction period, Dalton et al. (2018) found that the anterior medial hippocampus was engaged preferentially during the mental construction of scenes compared to arrays during fMRI.

Leveraging the high temporal resolution of MEG, in the current study we were able to directly examine the neural activity, particularly theta, associated with each specific construction phase, providing insights into how scenes and arrays were built step-by-step. In addition, we assessed interactions between our two regions of interest (ROIs), the anterior hippocampus and vmPFC, as mental imagery construction unfolded. Based on previous findings and models (McCormick et al., 2018; Ciaramelli et al., 2019; Barry et al., 2019) we predicted that these two brain regions would be preferentially engaged during scene, compared to array, construction, particularly at the initial phase while the scene was being set, and that vmPFC would drive hippocampal processing. Nevertheless, our paradigm was also capable of revealing if scenes and arrays were treated similarly by the hippocampus and vmPFC, supporting the argument that any form of associative processing should recruit these regions (Cohen and Eichenbaum, 1993; Yonelinas et al., 2019).

Materials and Methods

Participants

Twenty healthy, right-handed participants (13 female; mean age = 25.50 years; SD = 4.70) took part in the experiment. All participants gave written informed consent to participate in accordance with the University College London Research Ethics Committee. All were fluent English speakers with normal vision.

Stimuli and task procedure

During MEG scanning, participants performed two closely matched tasks adapted from Dalton et al (2018). Both tasks involved participants mentally constructing images with their eyes open while looking at a blank grey screen (Figure 1).

For the scene task, participants were asked to first imagine a 3D grid covering approximately the bottom two-thirds of the blank screen. They then heard three object descriptions, presented one at a time, and they imagined each object on the 3D grid, each in a separate location that was specified in advance by the trial cue (Figure 1). After the first object description, participants were instructed to imagine each subsequent object whilst continuing to maintain the image of the grid and previous object(s), without rearranging objects from their original cue-defined positions. By the final object description, the entire mental image created by participants was a simple scene composed of a 3D grid and three objects.

For the array task, participants were asked to first imagine a regular, flat 2D grid covering approximately the bottom two-thirds of the screen. They then heard three object descriptions, presented one at a time, and they imagined each object on the 2D grid, each in a separate location that was specified in advance by the trial cue (Figure 1). After the first object description, participants were instructed to imagine each subsequent object whilst continuing to maintain the image of the grid and previous object(s), without rearranging objects from their original cue-defined positions. By the final object description, the entire mental image created by participants was a set of three objects

on a flat 2D grid. In this array task it was emphasised to participants they should not link objects in a way that would create a scene.

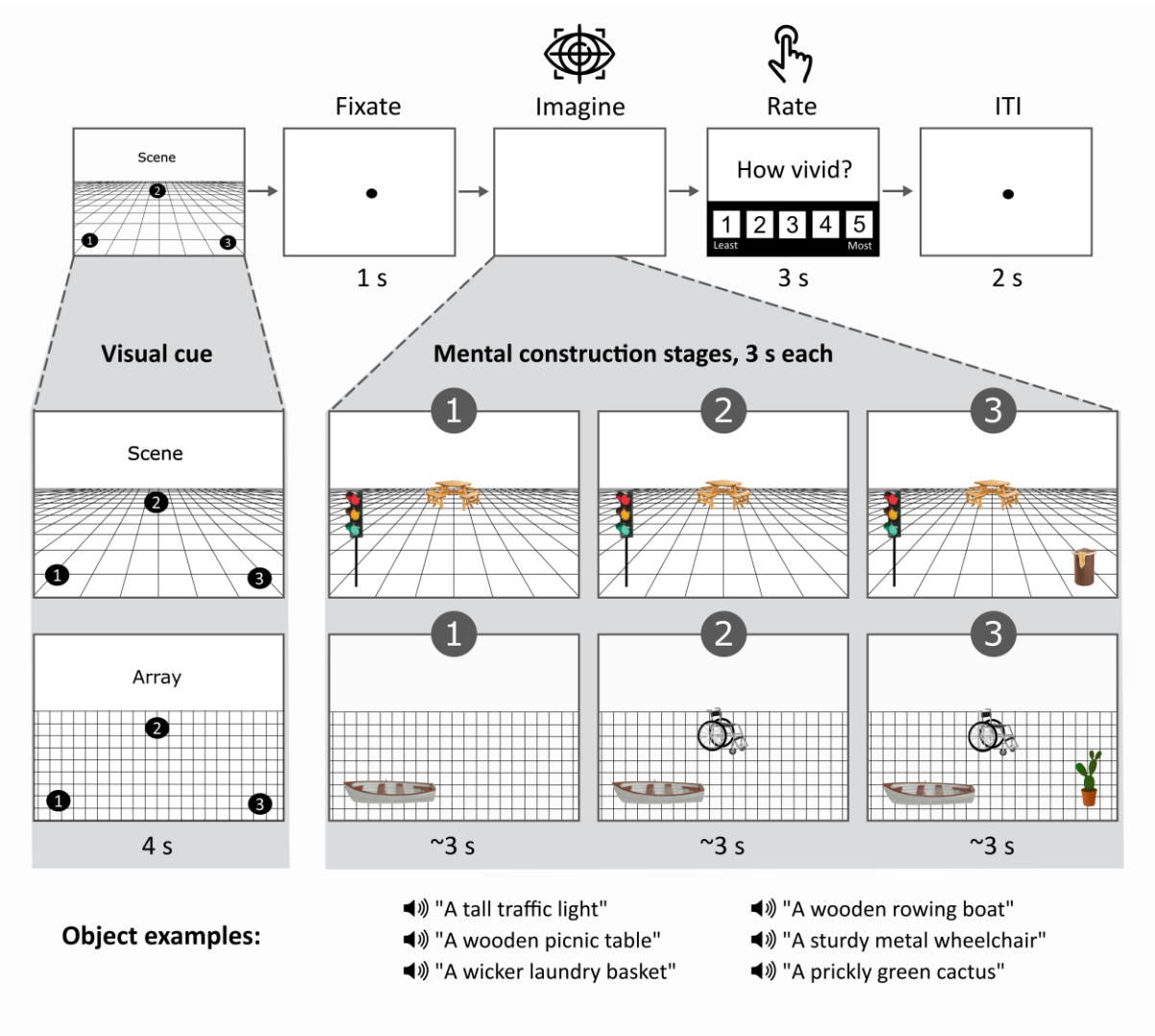

Figure 1. Structure of a trial. The top panel shows the timeline of, in this case, a scene trial. In the middle panels, an example cue configuration is shown on the left, and examples of what participants imagined as they constructed a scene or an array are shown on the right. Of note, during the construction stages, participants were looking at a blank screen. Examples of the auditorily presented object descriptions are provided in the bottom panel.

For both scene and array tasks, a visual cue determined the three specific locations where participants should imagine each object during a trial. There were four different cue configurations (Figure 2A) which were randomised across the experiment, and the frequency of each was matched across scene and array conditions. We emphasised the importance of following the cue configurations

as precisely as possible. This ensured matched eye movements between the scene and array conditions, consistency across participants, and that objects were imagined as separate and non-overlapping, occupying the full extent of the grid. Participants were asked to construct novel mental images of objects based on the descriptions alone, and not to rely on memories associated with the objects described, or to recall specific objects of their acquaintance. Additionally, they were told to imagine only the objects described and not add other elements to a scene or array. All imagery was to remain static and they were required to maintain a fixed viewpoint, as though looking at the image in front of them, rather than imagine moving parts of objects or imagine themselves moving through space.

The object descriptions were the same as those used by Dalton et al. (2018). Each description was heard only once. The objects were rated by a separate group of participants on a range of properties (Dalton et al., 2018), which enabled us to ensure that the scene and array conditions were closely matched in terms of the number and order of presentation of space-defining and space-ambiguous objects ($t_{(71)}$ = 0.497, p = 0.620) (Mullally and Maguire, 2011, 2013), ratings of object permanence ($t_{(71)}$ = 0.178, p = 0.859) (Mullally and Maguire, 2011), as well as the number of syllables in the objects descriptions ($t_{(71)}$ = 0.327, p = 0.745) and utterance duration ($t_{(71)}$ = 0.169, p = 0.866). Furthermore, all objects were rated as highly imageable, obtaining a score of at least 4 on a scale from 1 (not imageable) to 5 (extremely imageable). Objects in each triplet were not contextually or semantically related to each other. Object triplets were counterbalanced across conditions such that for some participants a triplet was in the scene condition and for others it was in the array condition. Importantly, and to reiterate, during both tasks participants viewed a blank screen, so there was no difference in visual input between conditions.

A third task was also included in the study. Participants heard a backward sequence of three numbers, after which they were instructed to mentally continue counting backwards. The primary function of this task was to provide participants with relief from the effortful imagination required of the scene and array trials. This counting task was not subject to analysis.

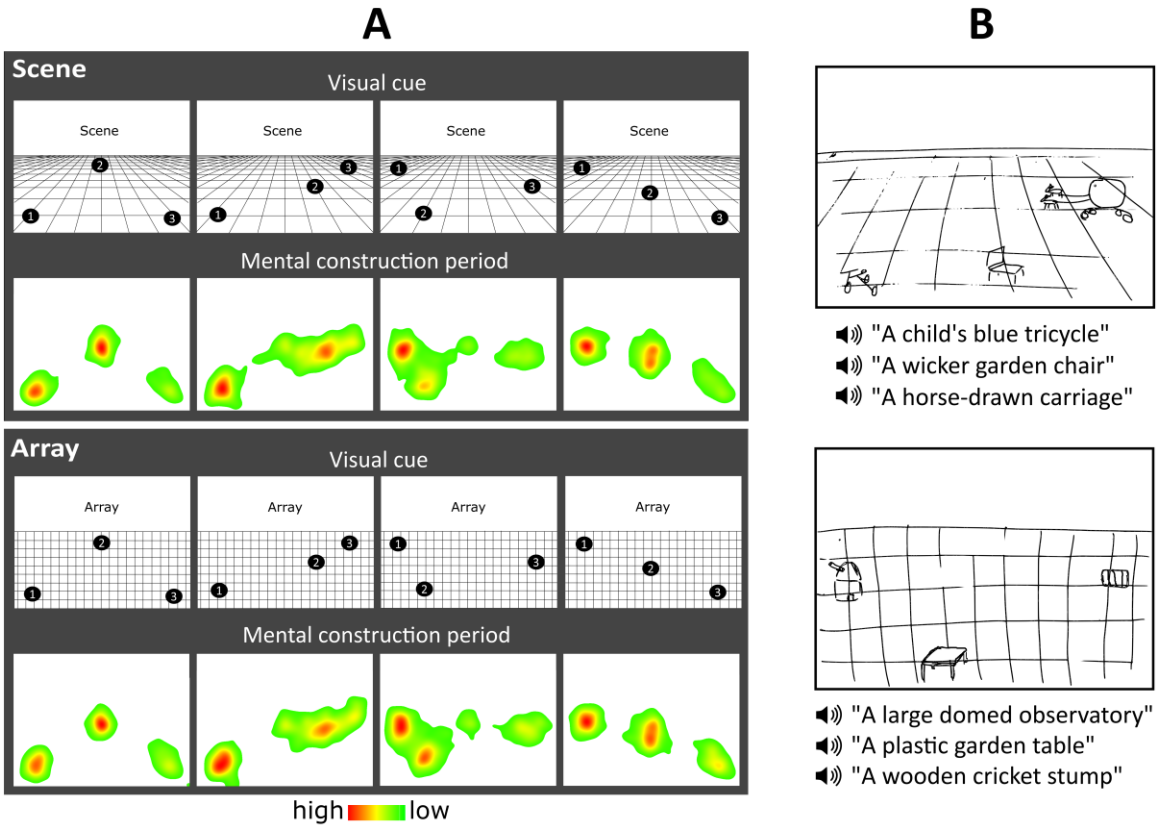

Figure 2. Eye movements and example drawings. ***A,*** Heat maps for each cue configuration for the scene and array tasks show the fixation count during the 9 s mental construction period. Each heat map is an aggregate of fixations on the blank screen across all trials for that cue configuration across all participants with eye tracking data (n=15). Red indicates higher fixation density and green lower fixation density. ***B,*** Pre-scan training drawings for the scene (top) and array (bottom) tasks from an example participant.

To summarise, scene and array tasks were identical except for one manipulation – imagining objects on a 3D grid induced a sense of depth and perspective, resulting in a mental representation of a scene, in contrast to imaging objects on a 2D grid which resulted in a mental representation of a non-scene array. This close matching of the scene with the array tasks meant any differences in neural activity could be attributed specifically to the mental construction of scenes within a 3D spatial layout, and not to more general mental construction processes. Moreover, the use of MEG meant that we could now examine the step-by-step construction of these representations with millisecond precision.

Pre-scan training

Before entering the scanner, participants were trained to become familiar with the task requirements. They completed four practice trials per task on a desktop computer in a darkened room, to liken the experience to that in the scanner environment. After each trial they rated the vividness of the mental imagery on a scale of 1 (not vivid at all) to 5 (extremely vivid). If they gave a rating of 3 or lower on any trial, the instructions and practice items were repeated. A score of 4 or more qualified them to proceed to the MEG experiment. After one practice trial per task, participants drew what they were able to imagine to further ensure task compliance (Figure 2B). Participants were excluded if they were unable to meet the vividness threshold, or drew representations that indicated a poor understanding of the task instructions.

MEG task timings

On each trial in the MEG scanner (Figure 1), a visual cue was presented for 4000 ms that contained both the identity of the task (scene or array) and the configuration of locations at which the objects should be imagined on the grid following each auditory object description. Following the cue, participants fixated on the centre of the screen for 1000 ms before the start of the imagination period (~15 seconds), during which they engaged in mental imagery whilst hearing three auditory object descriptions one after another delivered via MEG-compatible earbuds. Participants were instructed to move their eyes to where they were imagining each object on the screen. Each object description lasted approximately 2000 ms, followed by a silent 1000 ms gap before the presentation of the next object description, so that each object imagination period was 3000 ms in duration. These three construction stages were our main interest, and the focus of the data analyses. After the final object description, there was an additional 6000 ms silent period where participants maintained the image of the fully realised scene or array they had created, which was included in order to avoid an abrupt transition between trials. Participants then rated how vividly they were able to imagine the scene or array on that trial on a scale of 1 (not vivid at all) to 5 (extremely vivid), self-paced with a maximum

duration of 3000 ms. An inter-trial interval of 2000 ms preceded the next trial. The Cogent2000 toolbox for Matlab (http://www.vislab.ucl.ac.uk/cogent.php) was used to present stimuli and record responses in the MEG scanner.

A total of 24 trials per task were presented in a pseudorandomised order across four separate blocks – two blocks of twenty and two blocks of nineteen trials. To ensure participants attended to the tasks throughout scanning blocks, we included six catch trials (two per task, including the low level counting backwards task) pseudorandomly presented across all four scanning blocks. During a catch trial, participants were required to press a button when they heard a repeated object description or number within a triplet. The duration of each block was approximately six to seven minutes, an optimal time for participants to remain still and maintain attention during tasks. Participants were excluded if they repeatedly failed to make responses during the vividness rating period or catch trials.

In-scanner eye tracking

An Eyelink 1000 Plus (SR Research) eye tracking system with a sampling rate of 2000 Hz was used during MEG scanning to monitor task compliance. The right eye was used for both calibration and data acquisition, to record fixation eye tracking across the full screen. For some participants the calibration was insufficiently accurate, leaving 15 data sets in the eye tracking analyses.

Post-scan surprise memory test

Following the experiment, participants completed a surprise memory test for the scene and array tasks, outside of the scanner on a desktop computer. Participants were presented with all auditory object descriptions heard during the scanning experiment (72 scene and 72 array objects – 24 trials of each condition comprised of three objects each) and an additional 72 lure object descriptions not previously heard. The order of object descriptions was randomised. After hearing each description, participants pressed a button to indicate “yes” if they remembered hearing that object description during the scanning experiment or “no” if they did not. They then rated how confident they felt about

their answer on a scale from 1 (low confidence) to 5 (high confidence). Both responses were self-paced, with a maximum of 5000 ms for each.

Post-scan debriefing

Upon completion of the memory test, participants were asked about their experience of performing the scene and array tasks. Ratings completed during debriefing are reported in the Results (also see Table 1).

Analysis of behavioural data

Ratings for scene and array per-trial vividness during scanning were compared using paired-samples t-tests, as were the ratings from the post-scan debrief session. Eye tracking comparisons between scene and array tasks were performed using paired-samples t-tests to examine eye movements across the full 9000 ms construction period and, where relevant, using two-way repeated measures ANOVAs which assessed the effects of task (scene, array) and construction stage (first, second, third). For the post-scan surprise memory test, to determine whether memory for object descriptions was above chance for scenes and arrays, one-sample t-tests were performed. The memory test data were also analysed using two-way repeated measures ANOVAs which assessed the effects of task (scene, array) and construction stage (first, second, third). Statistical analyses were performed using SPSS version 25, using a significance threshold of $p < 0.05$.

MEG data acquisition

MEG data were acquired using a whole-head 275 channel CTF Omega MEG system within a magnetically shielded room, with a sampling rate of 1200 Hz. Participants were scanned in a seated position, with the back of their head resting on the back of the MEG helmet. Head position fiducial coils were attached to the three standard fiducial points (nasion, left and right preauricular) to monitor head position continuously throughout acquisition.

MEG data preprocessing

All continuous MEG data were high-pass filtered at 1 Hz, to eliminate slow drifts in signals from the MEG sensors. A stop-band filter was applied at 48-52 Hz to remove the power line interference, and a stop-band filter of 98-102 Hz to remove its first harmonic. Epochs corresponding to the three scene construction stages and three array construction stages were each defined as 0 to 3000 ms relative to the onset of each object description. Epochs corresponding to the scene and array pre-imagination fixation periods were defined as 0 to 1000 ms relative to the onset of the fixation period. Epochs were concatenated across trials for each condition and across scanning blocks.

MEG data analysis

MEG source reconstruction. Source reconstruction was performed using the DAiSS toolbox (https://github.com/SPM/DAiSS) implemented in SPM12 (www.fil.ion.ucl.ac.uk/spm). The linearly constrained minimum variance (LCMV) beamformer algorithm was used to generate maps of power differences between conditions at each construction stage. This type of beamformer uses weights that linearly map the MEG sensors to source space. Power is estimated at each source location whilst simultaneously minimising interference of contributions from other sources (Van Veen et al., 1997). This results in enhanced detection sensitivity of the target source activity. For each participant, a set of filter weights was built based on data from all six construction stages (three for scene and three for array) within the theta band (4-8 Hz) and a 0-3000 ms time window relative to object description onset. Coregistration to Montreal Neurological Institute (MNI) space was performed using a 5 mm volumetric grid and was based on nasion, left and right preauricular fiducials. The forward model was computed using a single-shell head model (Nolte, 2003).

At the first level, whole brain theta power was estimated within each construction stage for each condition, creating one weight-normalised image per construction stage per participant. The images were smoothed using a 12 mm Gaussian kernel. To determine the peak locations of power

differences between the scene and array tasks in our a priori ROIs, the anterior hippocampus and vmPFC, at the second level we performed a t-contrast at each of the three construction stages (for example, scene construction stage 1 relative to array construction stage 1). The search volume was then restricted to these regions by performing ROI analyses implemented in SPM12, using masks created with the AAL atlas in the WFU PickAtlas software (http://fmri.wfubmc.edu/software/pickatlas). As our a priori hypotheses pertained to the anterior hippocampus and vmPFC specifically, ROI analyses were performed using separate bilateral masks covering each of these regions. The vmPFC mask included Brodmann areas 10, 14, 25, and parts of areas 32, 11, 12 and 13. Additionally, for completeness, we also included a separate bilateral posterior hippocampal mask. We used a FWE corrected threshold of $p < 0.05$ and a spatial extent threshold of 10 voxels for each ROI. Source localised results were visualised using the MNI 152 T1 image in MRIcroGL (https://www.mccauslandcenter.sc.edu/mricrogl). Peaks in the hippocampus and vmPFC provided the seed regions for subsequent effective connectivity analyses. The beamformer analysis was also repeated in the alpha (9-12 Hz) and gamma (31-100 Hz) bands to examine whether effects of task at each stage were confined to the theta range.

To investigate whether engagement of the anterior hippocampus and vmPFC changed across the three construction stages during each condition, we used the same source extracted theta power obtained with the beamformer for an additional analysis. Using the previously defined masks (anterior hippocampus, vmPFC and posterior hippocampus), we extracted ROI-specific power values from each of the smoothed first level images. Power was subsequently averaged across each ROI, to produce an average for each participant at each of the six construction stages. Data from each ROI was entered into separate two-way repeated measures ANOVAs implemented in SPSS25, allowing us to evaluate changes in power between scene and array tasks and across construction stages (task × stage). Where the assumption of sphericity was violated using the Mauchly test, Greenhouse-Geisser corrected degrees of freedom were reported. Paired-sample t-tests were performed for each ROI in cases of a significant main effect or interaction, using a conservative significance level of $p < 0.01$. In order to

ascertain whether theta power originating from each ROI during task engagement corresponded to an increase or attenuation of power, we additionally extracted theta power from the 1000 ms fixation period immediately preceding the first construction stage of each trial. This followed the same source reconstruction protocol as the experimental conditions.

Effective connectivity. To assess how the hippocampus and vmPFC interacted during each of the three scene construction stages, we used Dynamic Causal Modelling (DCM) for cross spectral densities (Moran et al., 2009), which measured the magnitude of cross spectra between the ROIs. This connectivity approach permitted the comparison of biologically plausible models representing a priori hypotheses of the directed influence one region has over another, as well as mutual entrainment between regions (Friston, 2009; Kahan and Foltynie, 2013).

Electrophysiological DCMs use neural mass models that summarise the activity within a specified cluster of neurons. We employed a convolution-based local field potential biophysical model, used for EEG/MEG data (Moran et al., 2009; Moran et al., 2013; Barry et al., 2019). Intrinsic connectivity between different cell populations within a region are estimated. Extrinsic afferent inputs are categorised as forward, backward or lateral depending on which subpopulations these afferents project to (Felleman and Van Essen, 1991). Forward connections project to spiny stellate neurons in middle cortical layers, backward connections project to both excitatory pyramidal neurons and inhibitory interneurons, and lateral connections project to all cell populations.

Random-effects (RFX) Bayesian model selection (BMS) was then used to compare the evidence for different competing models that varied according to which connections were modulated by the experimental condition (Stephan et al., 2009). The RFX procedure does not assume the optimal model is the same across all participants, making it more accurate and robust against outliers than fixed-effects, since variability in brain activity across participants is to be expected when studying a complex cognitive process (Stephan et al., 2010). For each scene construction stage, we tested three models corresponding to the three hypotheses regarding hippocampal-vmPFC connectivity: (1)

hippocampus drives vmPFC, (2) vmPFC drives hippocampus, and (3) hippocampus and vmPFC are mutually entrained. When applied to our data, we determined the winning model to be the one with the greatest exceedance probability, which provides a measure of how likely one model is, compared to all other models across the group of participants as a whole. Evidence for each model was a balance between the goodness-of-fit of the model with how parsimonious an explanation it provided, using the minimum number of parameters possible.

Results

The goal of this study was to compare step-by-step scene construction with that of closely matched array construction, such that we could determine which brain regions supported specifically the construction of scenes whilst controlling for neural responses associated with objects, and general associative and constructive processes. We first examined the behavioural data to assess whether the participants adhered to the task instructions and to ascertain if there were any differences between the scene and array tasks that might have influenced the neural activity.

Did participants engage in the scene and array tasks and adhere to instructions?

Several methods were used to assess whether participants paid attention during scene and array trials, engaged in mental imagery, and complied with task-specific instructions throughout the experiment.

Pre-scan training. After performing scene and array practice trials during the pre-scan training, participants drew what they imagined on each trial, to ensure they could closely follow the task instructions and cue configurations. Scene and array drawings demonstrated participants formed the appropriate mental representations, and were able to mentally place the objects in the locations indicated by the cue configurations (see examples in Figure 2B).

Catch trials. Catch trials were included in each scanning block whereby participants were instructed to press a button whenever they heard a repeated object description (or number) within a trial. On average 98.33% (SD = 0.31) of catch trials were correctly identified, suggesting participants remained attentive throughout the experiment.

In-scanner eye tracking. Heat maps of the spatial pattern of fixations for the cue configurations confirmed not only remarkably close adherence to the instructions trial-by-trial, but also consistency across participants (Figure 2A). The eye tracking data were also examined for any differences between the scene and array tasks over the full 9000ms construction period, of which none were evident – fixation count ($t_{(14)}$ = 0.239, p = 0.814), fixation duration ($t_{(14)}$ = 0.559, p = 0.585), saccade count ($t_{(14)}$ = 0.322, p = 0.752), saccade amplitude ($t_{(14)}$ = 0.752, p = 0.465). We also examined the two fixation variables for any effects of task (scene, array) and construction stage (first, second, third). For both fixation count and fixation duration, there was no significant effect of task (fixation count: $F_{(1, 14)}$ = 1.441, p = 0.250; fixation duration: $F_{(1, 14)}$ = 2.964, p = 0.107) or construction stage (fixation count: $F_{(2, 28)}$ = 0.372, p = 0.693; fixation duration: $F_{(2, 28)}$ = 0.650, p = 0.530), and there was no significant task x construction stage interaction (fixation count: $F_{(2, 28)}$ = 2.394, p = 0.110; fixation duration: $F_{(2, 28)}$ = 0.356, p = 0.704). Eye movements were therefore closely matched across all construction stages, and there was no significant difference between the scene and array tasks.

Did vividness of mental imagery differ between scene and array tasks?

Participants rated the vividness of mental imagery immediately after each scene and array trial in the scanner on a scale of 1 (not vivid at all) to 5 (extremely vivid). On average, both scene (mean = 4.15, SD = 0.43) and array (mean = 4.08, SD = 0.49) trials were rated high on vividness, and there was no significant difference between the tasks ($t_{(19)}$ = 0.873, p = 0.394).

Were there any other subjective differences in mental imagery between the scene and array tasks?

After the experiment was completed, participants reported on their subjective experience of performing scene and array tasks in a debriefing session (questions and summary data are shown in Table 1). Mind-wandering was reported as very low for both scene and array tasks, and did not differ significantly between the two conditions ($t_{(19)} = 1.831$, $p = 0.083$). Mental imagery was performed with ease in both conditions ($t_{(19)} = 0.000$, $p = 1.000$). Participants also had no difficulty following the cue configuration instructions for either condition ($t_{(19)} = 1.000$, $p = 0.330$). As expected, scene trials were perceived as significantly more 3D than array trials, while arrays were rated as more 2D ($t_{(19)} = 17.168$, $p < 0.0001$). Participants also reported that they rarely needed to suppress scene-like mental imagery during array trials.

Table 1. Debrief ratings.

Question	**Rating (1-5 Likert scale)**	**Task**	**Mean ± SD**
To what degree did you feel your mind was wandering, that you were thinking of things other than the task?	1 = no mind wandering… 5= always mind wandering	Scene	1.20 ± 0.41
		Array	1.35 ± 0.49
How difficult was it to imagine the objects on the grid?	1 = easy…5 = very difficult	Scene	1.75 ± 0.64
		Array	1.75 ± 0.72
How difficult was it to follow the cue's instruction of where to imagine the objects on the grid?	1 = easy…5 = very difficult	Scene	1.2 ± 0.41
		Array	1.15 ± 0.37
Did you have any sense of 3D space during array trials? Please rate the extent to which you felt the image had a sense of depth.	1 = completely 2D… 5 = completely 3D	Scene	4.3 ± 0.44
		Array	1.55 ± 0.51
For the array trials, did you feel that you imagined the objects in a scene at all and tried to repress this?	1 = always repressed… 5 = never had to repress	Array	4.55 ± 0.60

SD = Standard Deviation.

Did memory performance differ between scene and array tasks?

After scanning, participants immediately engaged in a surprise item memory test. They performed above chance at recognising object stimuli from scene trials (mean = 84.31%, SD = 9.63; $t_{(19)} = 39.135$, $p < 0.0001$), array trials (mean = 85.42%, SD = 9.43; $t_{(19)} = 40.482$, $p < 0.0001$) and identifying novel items (mean = 87.54%, SD = 7.48; $t_{(19)} = 52.289$, $p < 0.0001$). Participants, therefore, paid sufficient attention during both tasks to successfully encode a large number of stimuli, even though they were never instructed to memorise. A repeated-measures ANOVA revealed no significant effect of task ($F_{(1, 19)} = 0.456$, $p = 0.508$), construction stage ($F_{(1.487, 28.262)} = 1.480$, $p = 0.240$), and no task x construction stage interaction ($F_{(1.554, 29.526)} = 0.739$, $p = 0.484$).

Having determined across a range of behavioural measures that the participants adhered to the task instructions, formed the appropriate mental images, with no differences in terms of key variables such as eye movements, vividness and memory performance between the scene and array tasks, we next examined the neural data.

MEG results

Our main ROIs were the anterior hippocampus and vmPFC, and our primary question was whether they would be preferentially engaged during the step-by-step construction of scenes.

Source space power differences for each construction stage separately. We first compared the scene and array tasks during each of the three construction stages. For the first stage we observed a significant attenuation of theta power in the scene relative to the array task in the left anterior hippocampus (peak x, y, z = -24, -20, -16; Figure 3A), left vmPFC (peak in BA32, -12, 40, -14; Figure 3A) and right vmPFC (peak in BA11, 16, 26, -18). The contrast of scene and array conditions during the second construction stage revealed an attenuation of theta activity for scenes in the vmPFC, extending bilaterally with an overall peak (-4, 26, -4) and subpeak (-12, 32, -18) in the left hemisphere (Figure

3A). No significant differences in anterior hippocampus or vmPFC were apparent between the scene and array tasks during the third construction stage. For completeness, no task-related theta power changes were found for any of the construction periods in the posterior hippocampus.

To investigate whether there were differences between scene and array tasks in frequencies other than theta, we performed the same analyses for alpha (9-12 Hz) and gamma (30-100 Hz) bands. No significant changes were evident in the anterior (or posterior) hippocampus or vmPFC.

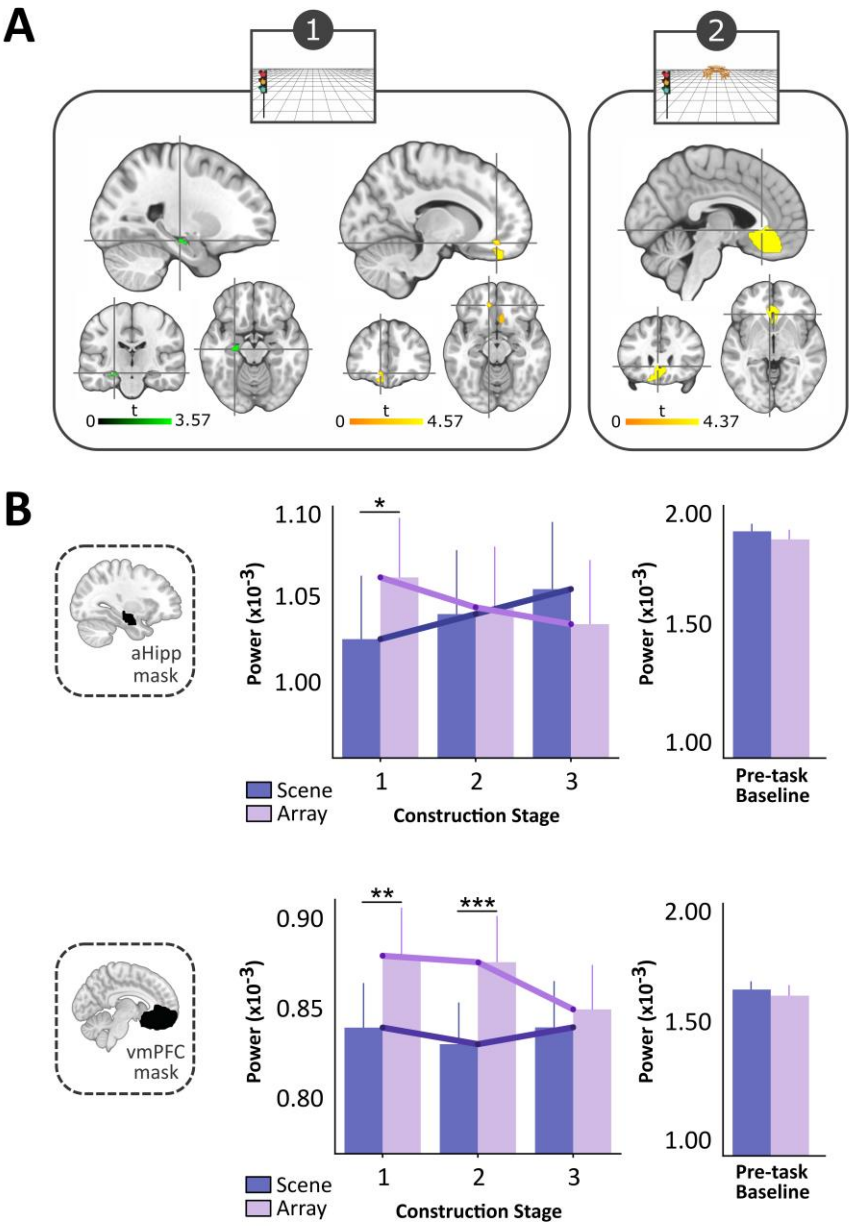

Figure 3. MEG results. ***A,*** Significant theta power changes within the anterior hippocampus (aHipp, shown in green) and ventromedial prefrontal cortex (vmPFC, shown in yellow) during scene relative to array construction (FWE $p < 0.05$, corrected for the ROI). Slices are centred on the overall peaks (crosshairs) in the left anterior hippocampus (x, y, z = -24, -20, -16) and left vmPFC (-12, 40, -14) during the first construction stage, and the vmPFC (-4, 26, -4) during the second period of construction. ***B,*** Task × construction stage interactions for theta power in the anterior hippocampus and vmPFC. For the hippocampus, power was significantly altered for the scene relative to the array condition during the first stage of construction. For the vmPFC, power was significantly changed for the scene compared to the array task for both the first and second construction periods. Relative to the pre-task baseline (bar plots on the right), theta power decreased during construction periods. *p = 0.014, **p = 0.008, ***p = 0.001. Error bars indicate ± 1 SEM.

Theta power changes across construction stages. Having observed between-task differences when each construction stage was considered separately, we next analysed the data in a different way to examine how theta activity changed across the construction stages. An ANOVA assessing the effects of task (scene, array) and construction stage (first, second, third) on anterior hippocampal activity revealed no significant effect of task ($F_{(1, 19)} = 0.694$, $p = 0.415$) or construction stage ($F_{(2, 38)} = 0.036$, $p = 0.965$), but a significant task × construction stage interaction ($F_{(2, 38)} = 5.762$, $p = 0.007$; Figure 3B). This was driven by the first construction stage of the scene task ($t_{(19)} = -2.713$, $p = 0.014$), indicating increased involvement of the anterior hippocampus during this scene stage, with engagement then decreasing over the subsequent two construction periods.

For the vmPFC, the ANOVA revealed a significant main effect of task ($F_{(1, 19)} = 17.252$, $p = 0.0005$; Figure 3B), but not of construction stage ($F_{(1.488, 28.272)} = 0.894$, $p = 0.392$), and there was no significant interaction ($F_{(2, 38)} = 2.586$, $p = 0.089$). The task effect was driven by theta power changes during the scene relative to the array task during both the first ($t_{(19)} = -2.959$, $p = 0.008$) and second ($t_{(19)} = -3.723$, $p = 0.001$) construction stages, indicating the greatest vmPFC involvement during these periods of the scene task.

We also considered whether the observed changes in theta power corresponded to increases or decreases by examining ROI power from the pre-task fixation period. Baseline theta power was higher compared to scene and array construction in anterior hippocampus and vmPFC, indicating that the scene-related task effects we observed in these brain regions represented power attenuation (Figure 3B).

Effective connectivity during the scene construction periods. The source localisation analyses described above established the peak locations of theta power changes in the anterior hippocampus and vmPFC during scene compared to array construction. We next examined the direction of information flow between these regions specifically during scene construction using DCM for cross spectral densities using the left hemisphere peaks in the anterior hippocampus and vmPFC identified

during the first construction stage (Figure 3A). We proposed three connectivity models based on established anatomical projections, representing the hypotheses for the hierarchical architecture of the hippocampus and vmPFC (Figure 4). The first model predicted hippocampal activity drove that of the vmPFC. Hippocampal projections via the fornix terminate in the middle layers of the ventral portion of the vmPFC (Aggleton et al., 2015), so this connection was classified as 'forward'. The second model specified the vmPFC as the influencing region. Connections from the vmPFC to the hippocampus are via the entorhinal cortex, where vmPFC inputs arrive at all cell populations (Rempl-Clower and Barbas, 2000), so were classified as 'lateral' connections. The third model predicted that the hippocampus and vmPFC drove each other through reciprocal connections (mutual entrainment), so both 'forward' and 'lateral' connections were specified. The approach adopted here to classifying DCM connections is also in line with previous work modelling hippocampal and vmPFC interactions in MEG (Barry et al., 2019). We then fit the models to each of the three 3000 ms scene construction stages.

The models were compared using random effects Bayesian model selection (BMS) to determine the winning model at each construction period at the group level (Figure 4). During the initial scene construction period, the model most likely to explain the data across all participants was the vmPFC driving anterior hippocampal activity, with an exceedance probability of 62.45%, almost double that for the mutual entrainment model (exceedance probability = 35.78%). Furthermore, there was very little evidence for the opposing model of the anterior hippocampus driving vmPFC (exceedance probability = 1.77%). During the second construction stage, the mutual entrainment model was the most probable, with an exceedance probability of 55.08%, compared to the hippocampus-driven model (exceedance probability = 31.18%) and the vmPFC-driven model (exceedance probability = 13.74%). During the third construction stage, the winning model was again the mutual entrainment model (exceedance probability = 73.32%) compared to the hippocampus-driven model (exceedance probability = 22.28%) and the vmPFC-driven model (exceedance probability = 4.40%). In summary, we found that the vmPFC drove hippocampal theta changes at the earliest stage

of scene construction, after which reciprocal connectivity between the regions underpinned the processing of additional scene elements.

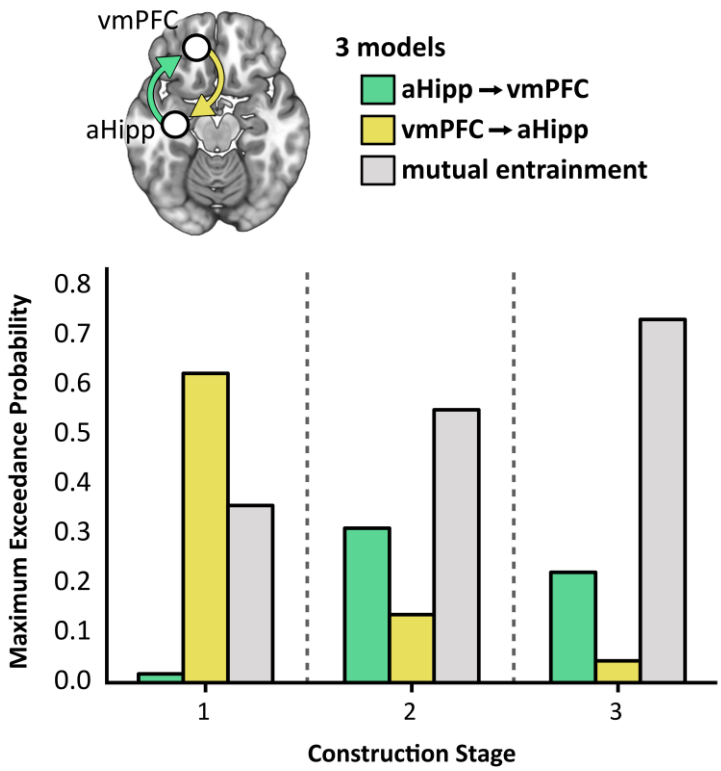

Figure 4. Connectivity between the anterior hippocampus (aHipp) and ventromedial prefrontal cortex (vmPFC) during step-by-step scene construction. Top panel, the three models of effective connectivity. Bottom panel, the results of Bayesian model selection revealed the model with the strongest evidence during construction stage 1 was the vmPFC driving anterior hippocampus, while for the latter two stages, there was stronger evidence for the anterior hippocampus and vmPFC driving each other through reciprocal connections (mutual entrainment).

Discussion

In this study we leveraged the fine temporal resolution of MEG to investigate the role of hippocampal and vmPFC neural dynamics in the step-by-step mental construction of scene and non-scene array imagery. Across three successive construction stages, we observed scene-related modulation of theta power in the anterior hippocampus during the initial stage, and in the vmPFC during the first two stages, relative to array construction. We also found that the scene-specific anterior hippocampal theta activity during the first phase of construction was driven by the vmPFC, with mutual entrainment between the two brain regions thereafter.

We observed attenuation in theta power for the scene relative to the array condition and consider this to reflect increased task-related neural activity. This is because power decreases in frequencies below 30 Hz during memory encoding have been inversely associated with the fMRI BOLD signal (Fellner et al., 2016), and related to enhanced subsequent memory recall (for reviews see Hanslmayr et al., 2012 and Herweg et al., 2020). Notably, our results mirror intracranial EEG studies, which consistently find decreases in theta during episodic memory (e.g. Fellner et al., 2019; Solomon et al., 2019), and a recent MEG study finding of attenuated anterior hippocampal theta whilst imagining scenes in response to single cue words (Barry et al., 2019).

Our primary interest in the comparison between scene and array tasks was to ascertain whether there was any specificity of engagement of the hippocampus and vmPFC. As predicted, both brain regions were preferentially recruited during the mental construction of scenes, corroborating the findings of Dalton et al. (2018) who used a similar scene-array comparison during fMRI, and extending the results of numerous previous fMRI (Hassabis et al., 2007b; Summerfield et al., 2010; Zeidman et al., 2015a, 2015b; Hodgetts et al., 2016; Zeidman and Maguire, 2016; Dalton and Maguire, 2017) and MEG (Kaplan et al., 2017; Barry et al., 2019) studies which documented scene-related hippocampal responses. Our scene and array tasks were very well matched, with no differences in stimulus properties, stimuli were counterbalanced across the two tasks, there were no disparities in eye movements, perceived task difficulty, attention, the vividness of mental imagery, and performance on a surprise memory test was also similar between the two conditions. Therefore, none of these factors can explain our neural findings. Moreover, because both scene and array tasks involved associations between objects and the construction of mental imagery, these processes per se could not have driven our effects. The most parsimonious explanation is that the anterior hippocampus and vmPFC may be particularly tuned to scenes. Why might this be the case?

Scene imagery seems to be important for, and is frequently deployed in the service of, hippocampal-dependent tasks including episodic memory, imagining the future and spatial navigation. For example, using a large sample (n = 217) of participants and multiple cognitive tests

with a wide spread of individual differences in performance, Clark et al. (2019a) reported that the ability to construct scene imagery explained the relationships between episodic memory, imagining the future and spatial navigation task performance. The prominence of scene imagery was further emphasised in another study involving the same sample, where the explicit strategies they used to perform episodic memory recall, future thinking and spatial navigation tasks was assessed (Clark et al., preprint). In each case, the use of scene visual imagery strategies was significantly higher than for all other types of strategies (see also Andrews-Hanna et al., 2010). The influence of scene imagery across cognition is perhaps not surprising, given that it mirrors how we perceive the world.

Our study design extended previous work by allowing us to examine changes in hippocampus and vmPFC engagement during each stage of construction rather than across the whole construction period (Dalton et al., 2018; Barry et al., 2019). We observed greater involvement of both the anterior hippocampus and vmPFC during the initial scene construction stage, when participants imagined the 3D grid and the first object, in contrast to construction of the equivalent array elements. Therefore, we have shown that these brain regions, known to support the construction of scene imagery, were engaged as soon as a single object was couched in a spatial context intended to form specifically a scene. In effect, the scene is 'set' early on.

It could be argued that the engagement of the anterior hippocampus and vmPFC during the initial stage of scene construction reflects encoding of novel stimuli. However, if novelty encoding was a primary influence, then a similar response should have been observed at each stage, and in both tasks, as the mental construction of novel objects was required throughout. Instead, we observed a change in hippocampal theta power specifically during the first scene stage, and then disengagement thereafter. Similarly, vmPFC activity was most prominent for the first two stages of scene, compared to array, construction. The success of encoding also does not explain our findings. There was no difference in performance in the post-scan surprise memory test for objects that were constructed first in scenes compared to those constructed first in arrays, or in the later stages of construction. This was also the case for eye movements.

An alternative explanation for our findings places the vmPFC in a supervisory role with respect to the hippocampus during the construction of scene imagery. It has been suggested that the vmPFC integrates ongoing episodic information into schematic knowledge structures (Van Kesteren et al., 2012; Gilboa and Moscovitch, 2017). Patients with damage to the vmPFC exhibit deficits consistent with aberrant schema re-activation (Gilboa et al., 2006; Ghosh et al., 2014). Similar to hippocampal-lesioned patients, they are also impaired at constructing scene imagery (Bertossi et al., 2016; De Luca et al., 2018), although this impairment is circumvented in vmPFC patients when they are provided with specific cues which enable them to describe individual scenes from episodic memories (Kurczek et al., 2015). This suggests a role for the vmPFC not in scene imagery construction itself, but rather in initiating endogenous processing necessary for scene construction.

Considering evidence such as this, McCormick et al. (2018; see also Ciaramelli et al., 2019) proposed a simple model of how the hippocampus and vmPFC might interact to produce scene imagery. In this architecture, vmPFC initiates the activation of schematic and other knowledge in neocortex that is relevant for a scene, whilst inhibiting elements that are not relevant. This information is conveyed to the hippocampus which constructs the scene. vmPFC then engages in iterations via feedback loops with neocortex and hippocampus to mediate the schema-based retrieval and monitoring necessary to flesh-out the scene, and to build the successive scenes that comprise the unfolding mental event such as an episodic memory.

Our findings are consistent with this view. The activation of schemas by vmPFC may provide an initial rudimentary template into which a scene may be constructed in collaboration with the hippocampus. Although our scene stimuli were composed of object triplets that were not contextually associated (van Kesteren et al., 2012), there is evidence for schema-guided construction of novel representations driven by the vmPFC (Garrido et al., 2015). Furthermore, the observed tonic response of the vmPFC throughout the first two construction stages in our study may reflect the prediction and preparatory processing necessary for the subsequent integration of scene elements (McCormick et al., 2018; Ciaramelli et al., 2019). Our analysis of effective connectivity revealed that during the first

stage of scene construction, the vmPFC drove activity in the anterior hippocampus, further supporting the perspective that the vmPFC instigates this process. After this initial scene-setting, hippocampal and vmPFC activity was mutually entrained, perhaps reflecting iterative feedback loops between them as each new object was integrated to form a fully realised scene (McCormick et al., 2018; Ciaramelli et al., 2019).

In conclusion, the hippocampus and vmPFC are particularly implicated in supporting cognitive functions such as episodic memory, imagining future events and spatial navigation. While it is likely these two brain areas participate in associative and constructive processing more generally (Dalton et al., 2018), here we have shown that their neural activity seems to be especially tuned to building scene representations, which some have argued may be the smallest functional building blocks of extended mental events (Ciaramelli et al., 2019). In future studies it will be important to elucidate the contributions of other brain regions, including posterior cortical areas (Dalton and Maguire, 2017), to this process and to characterise putative anatomical pathways that facilitate hippocampal-vmPFC interactions in the human brain. Moreover, if scenes are fundamental units of events, we need to understand how individual scenes are combined to construct the seamless dynamic unfolding episodes that constitute the memories of our past experiences.

References

Aggleton JP, Wright NF, Rosene DL, Saunders RC (2015) Complementary patterns of direct amygdala and hippocampal projections to the macaque prefrontal cortex. Cereb Cortex 25:4351–4373.

Aly M, Ranganath C, Yonelinas AP (2013) Detecting changes in scenes: The hippocampus is critical for strength-based perception. Neuron 78:1127–1137.

Andrews-Hanna JR, Reidler JS, Sepulcre J, Poulin R, Buckner RL (2010) Functional-anatomic fractionation of the brain's default network. Neuron 65:550–562.

Barry DN, Barnes GR, Clark IA, Maguire EA (2019) The neural dynamics of novel scene imagery. J Neurosci 39:4375– 4386.

Barry DN, Maguire EA (2019a) Remote memory and the hippocampus: A constructive critique. Trends Cogn Sci 23:128–142.

Barry DN, Maguire EA (2019b) Consolidating the case for transient hippocampal memory traces. Trends Cogn Sci 23:635–636.

Bertossi E, Aleo F, Braghittoni D, Ciaramelli E (2016) Stuck in the here and now: Construction of fictitious and future experiences following ventromedial prefrontal damage. Neuropsychologia 81:107–116.

Catani M, Dell'Acqua F, Thiebaut de Schotten M (2013) A revised limbic system model for memory, emotion and behaviour. Neurosci Biobehav Rev 37:1724–1737.

Catani M, Dell'Acqua F, Vergani F, Malik F, Hodge H, Roy P, Valabregue R, Thiebaut de Schotten M (2012) Short frontal lobe connections of the human brain. Cortex 48:273–291.

Ciaramelli E, De Luca F, Monk AM, McCormick C, Maguire EA (2019) What "wins" in VMPFC: Scenes, situations, or schema? Neurosci Biobehav Rev 100:208–210.

Clark IA, Hotchin V, Monk A, Pizzamiglio G, Liefgreen A, Maguire EA (2019a) Identifying the cognitive processes underpinning hippocampal-dependent tasks. J Exp Psychol Gen 148:1861–1881.

Clark IA, Monk AM, Maguire EA (preprint) Understanding strategy use during cognitive task performance. https://doi.org/10.1101/807990.

Clark IA, Maguire EA (2016) Remembering preservation in hippocampal amnesia. Annu Rev Psychol 67:51–82.

Cohen NJ, Eichenbaum H (1993) Memory, amnesia, and the hippocampal system. MIT Press.

Dalton MA, Maguire EA (2017) The pre/parasubiculum: A hippocampal hub for scene-based cognition? Curr Opin Behav Sci 17:34–40.

Dalton MA, Zeidman P, McCormick C, Maguire EA (2018) Differentiable processing of objects, associations, and scenes within the hippocampus. J Neurosci 38:8146–8159.

De Luca F, McCormick C, Mullally SL, Intraub H, Maguire EA, Ciaramelli E (2018) Boundary extension is attenuated in patients with ventromedial prefrontal cortex damage. Cortex 108:1–12.

Felleman DJ, Van Essen DC (1991) Distributed hierarchical processing in the primate cerebral cortex. Cereb Cortex 1:1–47.

Fellner MC, Gollwitzer S, Rampp S, Kreiselmeyr G, Bush D, Diehl B, Axmacher N, Hamer H, Hanslmayr S (2019) Spectral fingerprints or spectral tilt? Evidence for distinct oscillatory signatures of memory formation. PLoS Biol 17:e3000403.

Fellner MC, Volberg G, Wimber M, Goldhacker M, Greenlee MW, Hanslmayr S (2016) Spatial mnemonic encoding: Theta power decreases and medial temporal lobe BOLD increases co-occur during the usage of the method of loci. eNeuro 3:1–16.

Friston K (2009) Causal modelling and brain connectivity in functional magnetic resonance imaging. PLoS Biol 7:e1000033.

Garrido MI, Barnes GR, Kumaran D, Maguire EA, Dolan RJ (2015) Ventromedial prefrontal cortex drives hippocampal theta oscillations induced by mismatch computations. Neuroimage 120:362–370.

Ghosh VE, Moscovitch M, Colella BM, Gilboa A (2014) Schema representation in patients with ventromedial PFC lesions. J Neurosci 34:12057–12070.

Gilboa A, Alain C, Stuss DT, Melo B, Miller S, Moscovitch M (2006) Mechanisms of spontaneous confabulations: A strategic retrieval account. Brain 129:1399–1414.

Gilboa A, Moscovitch M (2017) Ventromedial prefrontal cortex generates pre-stimulus theta coherence desynchronization: A schema instantiation hypothesis. Cortex 87:16–30.

Graham KS, Barense MD, Lee ACH (2010) Going beyond LTM in the MTL: A synthesis of neuropsychological and neuroimaging findings on the role of the medial temporal lobe in memory and perception. Neuropsychologia 48:831–853.

Hanslmayr S, Staudigl T, Fellner M-C (2012) Oscillatory power decreases and long-term memory: The information via desynchronization hypothesis. Front Hum Neurosci 6:1–20.

Hassabis D, Kumaran D, Vann SD, Maguire EA (2007a) Patients with hippocampal amnesia cannot imagine new experiences. Proc Natl Acad Sci U S A 104:1726–1731.

Hassabis D, Kumaran D, Maguire EA (2007b) Using imagination to understand the neural basis of episodic memory. J Neurosci 27:14365–14374.

Hassabis D, Maguire EA (2007) Deconstructing episodic memory with construction. Trends Cogn Sci 11:299–306.

Hodgetts CJ, Shine JP, Lawrence AD, Downing PE, Graham KS (2016) Evidencing a place for the hippocampus within the core scene processing network. Hum Brain Mapp 37:3779–3794.

Kahan J, Foltynie T (2013) Understanding DCM: Ten simple rules for the clinician. Neuroimage 83:542–549.

Kaplan R, Bush D, Bisby JA, Horner AJ, Meyer SS, Burgess N (2017) Medial prefrontal–medial temporal theta phase coupling in dynamic spatial imagery. J Cogn Neurosci 29:507–519.

Kurczek J, Wechsler E, Ahuja S, Jensen U, Cohen NJ, Tranel D, Duff M (2015) Differential contributions of hippocampus and medial prefrontal cortex to self-projection and self-referential processing. Neuropsychologia 73:116–126.

Lee ACH, Buckley MJ, Pegman SJ, Spiers H, Scahill VL, Gaffan D, Bussey TJ, Davies RR, Kapur N, Hodges JR, Graham KS (2005) Specialization in the medial temporal lobe for processing of objects and scenes. Hippocampus 15:782–797.

Maguire EA, Mullally SL (2013) The hippocampus: A manifesto for change. J Exp Psychol Gen 142:1180–1189.

McCormick C, Ciaramelli E, De Luca F, Maguire EA (2018) Comparing and contrasting the cognitive effects of hippocampal and ventromedial prefrontal cortex damage: A review of human lesion studies. Neuroscience 374:295–318.

Moran R, Pinotsis DA, Friston K (2013) Neural masses and fields in dynamic causal modeling. Front Comput Neurosci 7:57.

Moran RJ, Stephan KE, Seidenbecher T, Pape HC, Dolan RJ, Friston KJ (2009) Dynamic causal models of steady-state responses. Neuroimage 44:796–811.

Mullally SL, Intraub H, Maguire EA (2012) Attenuated boundary extension produces a paradoxical memory advantage in amnesic patients. Curr Biol 22:261–268.

Mullally SL, Maguire EA (2011) A new role for the parahippocampal cortex in representing space. J Neurosci 31:7441–7449.

Mullally SL, Maguire EA (2013) Exploring the role of space-defining objects in constructing and maintaining imagined scenes. Brain Cogn 82:100–107.

Nolte G (2003) The magnetic lead field theorem in the quasi-static approximation and its use for magnetoenchephalography forward calculation in realistic volume conductors. Phys Med Biol 48:3637–3652.

O'Keefe J, Dostrovsky J (1971) The hippocampus as a spatial map. Preliminary evidence from unit activity in the freely-moving rat. Brain Res 34:171–175.

Rempl-Clower NL, Barbas H (2000) Laminar pattern of connections between prefrontal and anterior temporal cortices in the rhesus monkey is related to cortical structure and function. Cereb Cortex 10:851–865.

Schacter DL, Addis DR (2007) On the constructive episodic simulation of past and future events. Behav Brain Sci 30:330–332.

Scoville WB, Milner B (1957) Loss of recent memory after bilateral hippocampal lesions. J Neurol Neurosurg Psychiatry 20:11–21.

Solomon EA, Stein JM, Das S, Gorniak R, Sperling MR, Worrell G, Inman CS, Tan RJ, Jobst BC, Rizzuto DS, Kahana MJ (2019) Dynamic theta networks in the human medial temporal lobe support episodic memory. Curr Biol 29:1100-1111.e4.

Stephan KE, Penny WD, Daunizeau J, Moran RJ, Friston KJ (2009) Bayesian model selection for group studies. Neuroimage 46:1004–1017.

Stephan KE, Penny WD, Moran RJ, den Ouden HEM, Daunizeau J, Friston KJ (2010) Ten simple rules for dynamic causal modeling. Neuroimage 49:3099–3109.

Summerfield JJ, Hassabis D, Maguire EA (2010) Differential engagement of brain regions within a "core" network during scene construction. Neuropsychologia 48:1501–1509.

Van Kesteren MTR, Ruiter DJ, Fernández G, Henson RN (2012) How schema and novelty augment memory formation. Trends Neurosci 35:211–219.

Van Veen BD, Van Drongelen W, Yuchtman M, Suzuki A (1997) Localization of brain electrical activity via linearly constrained minimum variance spatial filtering. IEEE Trans Biomed Eng 44:867–880.

Yonelinas AP, Ranganath C, Ekstrom AD, Wiltgen BJ (2019) A contextual binding theory of episodic memory: Systems consolidation reconsidered. Nat Rev Neurosci 20:364–375.

Zeidman P, Lutti A, Maguire EA (2015a) Investigating the functions of subregions within anterior hippocampus. Cortex 73:240–256.

Zeidman P, Maguire EA (2016) Anterior hippocampus: The anatomy of perception, imagination and episodic memory. Nat Rev Neurosci 17:173–182.

Zeidman P, Mullally SL, Maguire EA (2015b) Constructing, perceiving, and maintaining scenes: Hippocampal activity and connectivity. Cereb Cortex 25:3836–3855.